

Nuclear Moment Ratios in ^{237}Np from Mössbauer Spectra*

J. A. STONE AND W. L. PILLINGER

Savannah River Laboratory, E. I. du Pont de Nemours and Company, Aiken, South Carolina

(Received 17 July 1967)

Hyperfine structure has been observed in Mössbauer spectra of the 59.54-keV γ ray of ^{237}Np in NpAl_2 and NpCl_4 . At 77°K, NpAl_2 gave an unsplit absorption line; at 4.2 and 2.35°K, magnetic hfs extending over ≈ 18 cm/sec was observed. The partially resolved spectrum of NpCl_4 at 77°K was interpreted as pure quadrupole splitting; at 4.2°K, combined magnetic and quadrupole interactions were found. From these spectra, the following ratios were determined between the 59.54-keV level and the ground state of ^{237}Np : quadrupole-moment ratio $+1.0 \pm 0.1$; magnetic-moment ratio $+0.537 \pm 0.005$. Nuclear polarization in the Mössbauer spectra of NpAl_2 at 4.2 and 2.35°K enabled the magnetic-moment ratio to be determined uniquely. The results agree with theoretical predictions of the collective model if the odd-nucleon g factor is quenched to about 70% of the free-proton value. From a comparison of the present work with earlier measurements, a new estimate for the ^{237}Np ground-state magnetic moment is 2.8 nm.

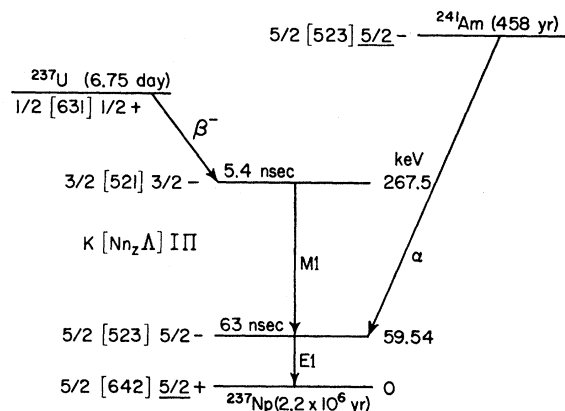
INTRODUCTION

THE Mössbauer spectra of the 59.54-keV γ transition in ^{237}Np in the compounds NpAl_2 and NpCl_4 were obtained at 4.2 and 77°K. From hyperfine structure observed in these spectra, the ratio of the nuclear quadrupole moments κ and the ratio of the nuclear magnetic moments ρ between the 59.54-keV level and the ground state of ^{237}Np were deduced. These results can be compared with nuclear systematics and form a basis for further development of solid-state and chemical information, using the Mössbauer effect in this isotope. Earlier work^{1,2} demonstrated the ^{237}Np Mössbauer effect with NpO_2 , following both β decay of ^{237}U and α decay of ^{241}Am ; an unsplit line was found that was many times broader than natural linewidth. In the present work, resolved hyperfine spectra were obtained because of the large extranuclear fields in NpAl_2 and NpCl_4 , even though linewidths were not significantly narrower.

The nuclear properties of the ^{237}Np 59.54-keV γ transition³⁻⁵, as shown in the partial decay scheme, Fig. 1, are favorable for recoilless emission and absorption. The half-life of the 59.54-keV excited state⁶ is 63 nsec, giving a Mössbauer linewidth (2Γ) of 0.007 cm/sec; this is potentially one of the sharpest lines available for Mössbauer studies. The average recoil energy of the 59.54-keV transition is 8×10^{-3} eV or about four times greater than that of the Mössbauer transitions in ^{57}Fe and ^{119}Sn , so that somewhat smaller recoilless fractions are expected. This γ ray belongs to

a class of anomalous $E1$ transitions between different intrinsic states in deformed nuclei.⁷ These transitions are characterized by unusually long lifetimes and small internal conversion coefficients; in this case, the total conversion coefficient is 1.0, so that half the transitions result in 59.54-keV photons. Finally, the transition proceeds to the ground state of a long-lived isotope, which is available in gram quantities. Thus ^{237}Np meets the principal criteria for Mössbauer nuclei.

The spins of both the ground state and the 59.54-keV level of ^{237}Np are $\frac{5}{2}$. The splitting of these levels in an axially symmetric electric field gradient or a magnetic field is illustrated schematically in Fig. 2. For dipole radiation, the allowed γ transitions between the sublevels have $\Delta m_I = 0, \pm 1$. Quadrupole splitting gives three sublevels for each state, with seven allowed γ lines; magnetic splitting gives six sublevels for each state, with 16 allowed γ lines. The order and spacing of these γ lines depends upon the relative magnitudes and signs of the nuclear moments for the two states. The hyperfine pattern is therefore directly related to the nuclear moment ratios, κ and ρ ; this relationship is discussed in detail in the following sections.

FIG. 1. Partial decay scheme to levels of ^{237}Np .

⁷ F. Asaro, F. S. Stevens, J. M. Hollander, and I. Perlman, *Phys. Rev.* **117**, 492 (1960).

* The information contained in this article was developed during the course of work under U. S. Atomic Energy Commission Contract No. AT(07-2)-1.

¹ J. A. Stone and W. L. Pillinger, *Phys. Rev. Letters* **13**, 200 (1964).

² J. A. Stone, in *Applications of the Mössbauer Effect in Chemistry and Solid-State Physics* (International Atomic Energy Agency, Vienna, 1966), p. 179.

³ J. O. Rasmussen, F. L. Canavan, and J. M. Hollander, *Phys. Rev.* **107**, 141 (1957).

⁴ C. M. Lederer, J. K. Poggenburg, F. Asaro, J. O. Rasmussen, and I. Perlman, *Nucl. Phys.* **84**, 481 (1966).

⁵ T. Yamazaki and J. M. Hollander, *Nucl. Phys.* **84**, 505 (1966).

⁶ J. K. Beling, J. O. Newton, and B. Rose, *Phys. Rev.* **87**, 670 (1952).

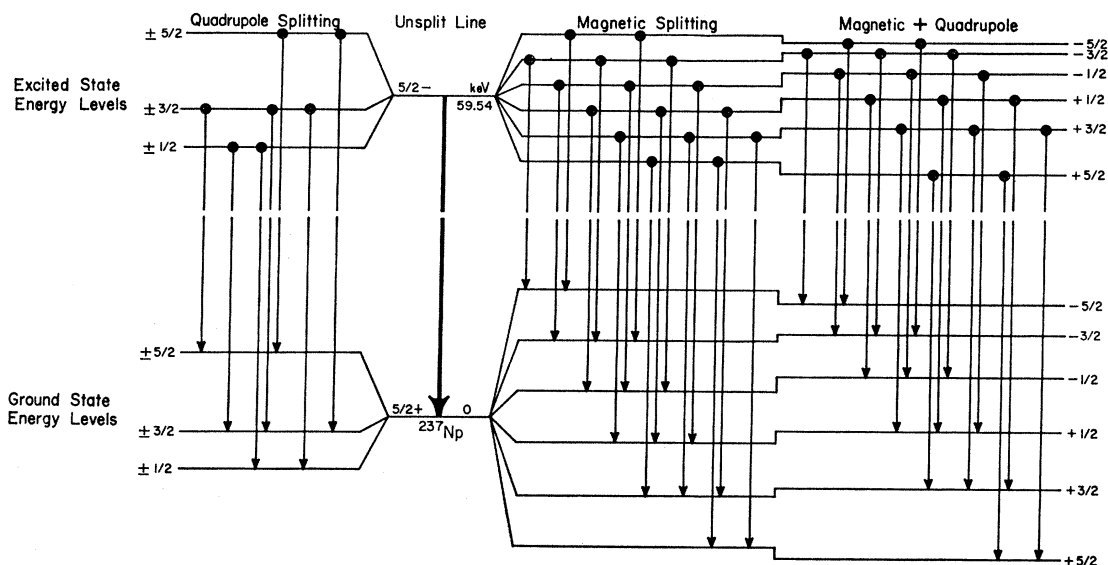


Fig. 2. Magnetic and quadrupole splitting of the spin $\frac{5}{2}$ ground state and 59.54-keV level of ^{237}Np . The hyperfine γ lines allowed for an $E1$ transition are shown for each case.

The purpose of this paper is to give the nuclear-moment information obtained from Mössbauer experiments with ^{237}Np ; solid-state and chemical aspects of the data will be discussed in a subsequent publication. The results of the Mössbauer measurements are presented, together with a theoretical analysis giving the nuclear-moment ratios. Because the result for ρ is double-valued, additional experimental evidence is presented to permit selection of the proper value. These experimental results are then compared with nuclear theory and with other measurements found in the literature.

EXPERIMENTAL METHOD AND MATERIALS

Velocity spectra were taken with a standard loud-speaker-type Mössbauer spectrometer⁸ using a constant-acceleration drive (triangular velocity wave form) and employing a 400-channel analyzer operated in the multiscaler mode. Velocity calibration was achieved by a careful study of the behavior of line positions as a function of peak-driving voltage, and at the lower velocities by ^{57}Fe reference spectra; the measured velocities are expected to be accurate to better than 0.5%. The determination of nuclear-moment ratios is independent of velocity calibration. The γ -ray detector was a proportional counter filled with a 90% Kr–10% CH_4 mixture. The window of the single-channel analyzer was set to accept both the 59.54-keV photopeak and its escape peak.

The cryogenic system has been described previously.² In each experiment, the source and absorber were at the same temperature, either 4.2°K with liquid helium or

77°K with liquid nitrogen. One experiment was performed at 2.35°K by pumping on the liquid-helium bath; temperature was determined from vapor-pressure measurements.

Sources of 6.75-day ^{237}U produced by thermal-neutron irradiation of enriched ^{236}U were used in the form of 1% solid solutions of UO_2 in NpO_2 . Several sources of this type previously have been prepared; their behavior with respect to linewidth, isomer shift, and recoilless efficiency, as determined with a reference NpO_2 absorber, is reproducible. The data reported in this paper were obtained with two such sources.

The intermetallic compound NpAl_2 was prepared by reaction of stoichiometric quantities of the metals at 700°C in an inert atmosphere⁹; the composition was confirmed by x-ray powder patterns. An absorber containing ≈ 100 mg/cm² ^{237}Np was fabricated from this material. NpAl_2 has the cubic, Laves-phase crystal structure $Fd\bar{3}m$, O_h^7 , which should give a vanishing lattice contribution to the electric field gradient at the Np nucleus.

Anhydrous NpCl_4 was prepared¹⁰ by reaction of NpO_2 with CCl_4 vapor at 500°C. The encapsulated absorber material underwent slow decomposition, with the Cl/Np atom ratio changing from 4.0 to 2.8; over a period of months, the Mössbauer spectrum also changed from a well-resolved hyperfine pattern to a single broad line. However, freshly prepared material was pure NpCl_4 as determined by chemical analysis and x-ray powder patterns; absorbers made at different times from fresh batches gave reproducible Mössbauer spectra. Two absorbers, each ≈ 100 mg/cm² of ^{237}Np , from different batches of material, were required to

⁸ E. Kankeleit, Rev. Sci. Instr. 35, 194 (1964).

⁹ O. J. C. Runnalls, J. Metals 5, 1460 (1953).

¹⁰ S. Fried and N. Davidson, J. Am. Chem. Soc. 70, 3539 (1948).

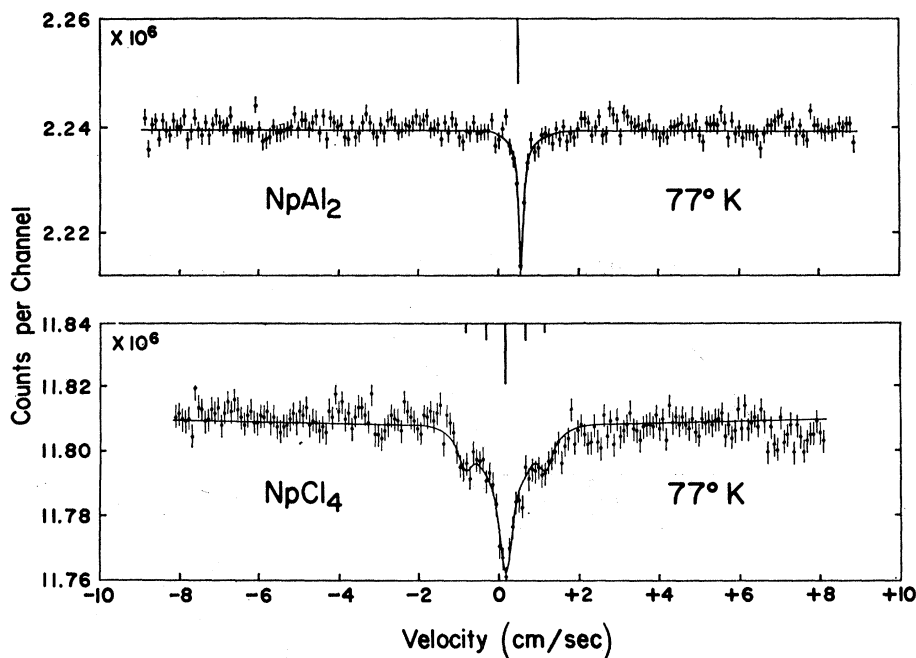


FIG. 3. Velocity spectra of NpAl_2 and NpCl_4 at 77°K . Source was ^{237}U in NpO_2 . Solid curves through the data points are least-squares fits of the theoretical patterns shown above each spectrum.

obtain the data reported here. NpCl_4 has a tetragonal crystal structure¹¹ $I4/amd$, D_{4h}^{19} , which should give a nonvanishing electric field gradient with axial symmetry at the Np nucleus.

Data taken with the time-mode experimental arrangement were in the form of duplicate, mirror-image velocity spectra; counts stored in one half of the channels corresponded to motion of the source away from the absorber, while those stored in the other half corresponded to motion toward the absorber. The two spectra were superimposed upon a nonlinear base line due to the changing solid angle between source and detector. In the analysis of the data, this solid-angle effect was removed by adding together the two velocity spectra; the solid-angle effect is a source of instrumental line broadening, but does not influence the line positions. Line positions were determined precisely with the aid of a computer, using the variable-metric method¹² for least-squares curve fitting.

EXPERIMENTAL RESULTS

Quadrupole-Moment Ratio

Velocity spectra at 77°K for NpAl_2 and NpCl_4 are shown in Fig. 3, with numerical results obtained from least-squares analysis of the spectra included in Table I. At this temperature, NpAl_2 gives a single, unsplit line, consistent with its cubic structure; NpCl_4 gives a symmetric, poorly resolved spectrum consisting of a strong central resonance, somewhat broader than the NpAl_2 line, with satellite resonances to either side. The NpCl_4 spectrum can be interpreted as pure quadrupole splitting with an axially symmetric field gradient; and by comparison of the experimental pattern with calculated hyperfine patterns, the quadrupole-moment ratio κ can be obtained. Calculation of hyperfine patterns for quadrupole splitting, as a function of κ , is described below.

The quadrupole interaction partially removes the degeneracy of a nuclear state; for axial symmetry, the

TABLE I. Measured hyperfine-structure parameters for NpAl_2 and NpCl_4 .

Absorber	Temperature ($^\circ\text{K}$)	$g_0\mu_n H_{\text{eff}}$ (cm/sec) ^a	$g_1\mu_n H_{\text{eff}}$ (cm/sec) ^a	$\frac{1}{2}eqQ^b$ (cm/sec) ^a	Isomer shift ^c (cm/sec)
NpAl_2	4.2	$+5.34 \pm 0.05$	$+2.85 \pm 0.05$	$+0.05 \pm 0.05$	$+0.57 \pm 0.05$
NpAl_2	77			< 0.30	$+0.56 \pm 0.05$
NpCl_4	4.2	$+4.74 \pm 0.05$	$+2.54 \pm 0.05$	-0.42 ± 0.05	$+0.22 \pm 0.05$
NpCl_4	77			0.88 ± 0.05	$+0.17 \pm 0.05$

^a For the 59.54-keV γ ray of ^{237}Np , $1 \text{ cm/sec} = 480.2 \text{ Mc/sec}$.

^b Values for quadrupole splitting at 4.2°K are $\frac{1}{2}eqQ(\frac{2}{3}\cos^2\theta - \frac{1}{3})$, where θ is the angle between the magnetic and electric field axes; at 77°K , the value given are $|\frac{1}{2}eqQ|$.

^c With respect to NpO_2 .

¹¹ W. H. Zachariasen, Acta Cryst. 2, 388 (1949).

¹² W. C. Davidon, Argonne National Laboratory Report No. ANL-5990 (Rev.), 1959 (unpublished).

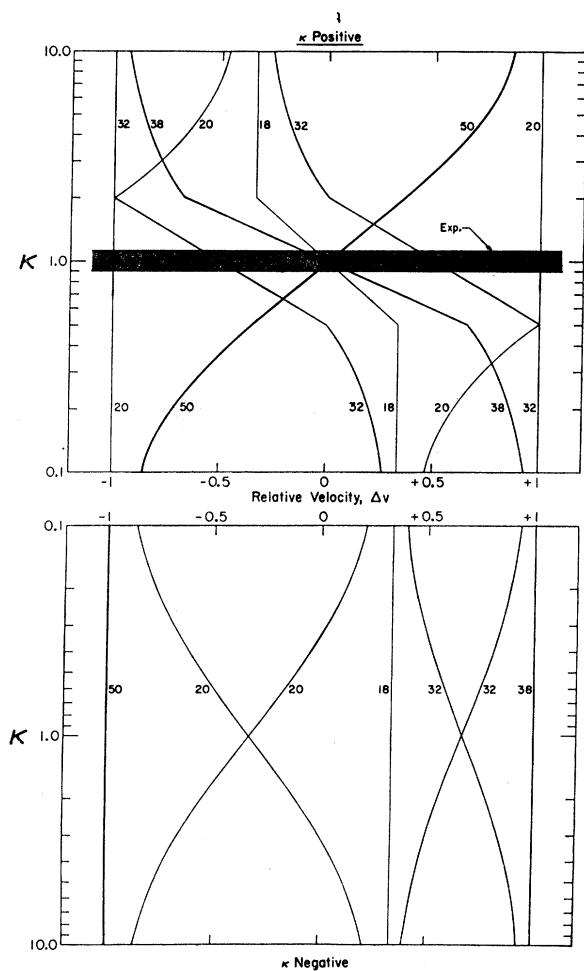


FIG. 4. Hyperfine line positions for $\frac{5}{2} \rightarrow \frac{5}{2}$ transitions with quadrupole splitting in an axial electric field gradient, as a function of the quadrupole-moment ratio κ . Relative intensities are indicated for each line. The diagram shown holds for $\frac{1}{4}eqQ_0$ positive; for negative $\frac{1}{4}eqQ_0$ the mirror image about zero velocity is correct. The shaded region gives hyperfine patterns which fit the experimental spectrum for NpCl_4 at 77°K .

energy of the sublevels (relative to the energy of the unsplit state) is given by the expression

$$W_Q(m) = \frac{1}{4}eqQ \left[\frac{3m^2 - I(I+1)}{I(2I-1)} \right] = \left(\frac{1}{4}eqQ \right) B(m)$$

where Q is the quadrupole moment of the state and $\frac{1}{4}eqQ$ is the quadrupole coupling constant. For $I = \frac{5}{2}$, the coefficients $B(m)$ are

$$B(\pm\frac{5}{2}) = +1.0, \quad B(\pm\frac{3}{2}) = -0.2, \quad B(\pm\frac{1}{2}) = 0.8.$$

Let the subscript 1 refer to the nuclear excited state and subscript 0 the ground state. Then, the energies of γ lines between sublevels of an excited state with $I = \frac{5}{2}$ (such as the 59.54-keV state of ^{237}Np) and the ground state with $I = \frac{5}{2}$, relative to the unsplit γ -ray energy, are

given by the set of linear equations

$$E_Q(m_1; m_0) = B(m_1)\kappa - B(m_0) \quad \text{for } m_1 - m_0 = 0, \pm 1,$$

in units of the ground-state quadrupole coupling constant, $\frac{1}{4}eqQ_0$, where $\kappa = Q_1/Q_0$.

For comparison with experiment, it is convenient to transform the transition energies to a normalized scale ranging from -1 to $+1$. As κ varies, different pairs of transitions give E_{\min} and E_{\max} , due to crossovers. The new set of transition-energy equations is given by the transformation

$$E_Q'(m_1; m_0) = (E_{\max} - E_{\min})^{-1} \times [2E_Q(m_1; m_0) - E_{\max} - E_{\min}].$$

Complete sets of these relative-energy expressions for all ranges of κ may be found in Ref. 2. Calculated relative positions of the seven hyperfine lines between quadrupole-split states with $I_1 = I_0 = \frac{5}{2}$ are presented in Fig. 4 as a function of κ . A logarithmic scale for κ is used to display features which are invariant upon the interchange of Q_1 with Q_0 . The relative intensities shown are proportional to the squares of Clebsch-Gordan coefficients.

Figure 4 shows that, in general, hyperfine patterns for quadrupole splitting are not symmetric, nor do they have a strong centrally located line, except for $\kappa \approx +1$ (equal quadrupole moments). The ratio of the quadrupole moment of the 59.54-keV level of ^{237}Np to that of the ground state is measured as

$$\kappa = +1.0 \pm 0.1.$$

The result for κ is corroborated in the velocity spectrum of NpCl_4 at 4.2°K as discussed in the following section.

Magnetic-Moment Ratio

Velocity spectra at 4.2°K for NpAl_2 and NpCl_4 are shown in Fig. 5, with the numerical results given in Table I. Numerous resonance lines, which are attributed to magnetic splitting, were observed over a wide velocity range with both materials. In the NpAl_2 spectrum, the line positions are symmetric about the center of the hyperfine pattern, a characteristic of pure magnetic splitting; from this pattern, the magnetic-moment ratio ρ can be obtained. The spectrum of NpCl_4 shows the effect of combined magnetic and quadrupole interactions. Calculated magnetic hyperfine patterns are obtained in a manner analogous to that for quadrupole splitting.

The degeneracy of a nuclear state is completely removed by the magnetic interaction to give sublevels whose relative energies are

$$W_M(m) = g\mu_n H_{\text{eff}} m,$$

where g is the gyromagnetic ratio μ/I of the level, and H_{eff} is the effective magnetic field at the nucleus. The energies of γ lines between sublevels of an excited state

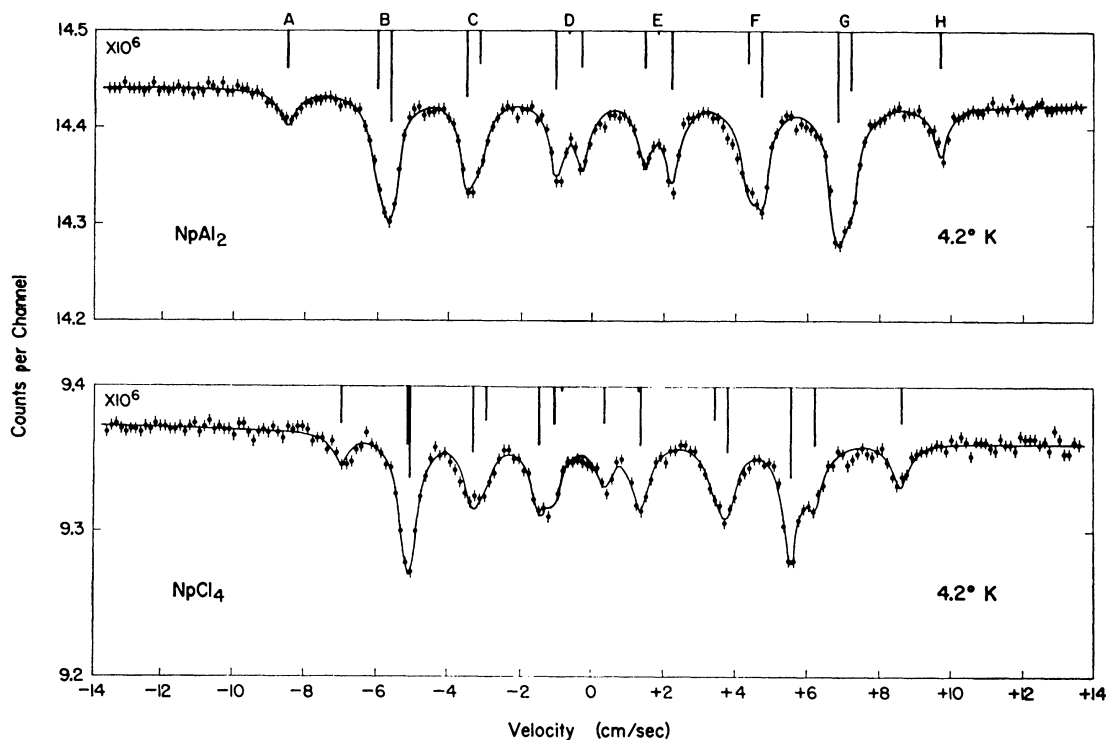


FIG. 5. Velocity spectra of NpAl_2 and NpCl_4 at 4.2°K . Source was ^{237}U in NpO_2 . Solid curves through the data points are least-squares fits of the theoretical patterns shown above each spectrum.

and the ground state, relative to the unsplit γ -ray energy, are given by the set of linear equations

$$E_M(m_1; m_0) = m_1\rho - m_0 \quad \text{for } m_1 - m_0 = 0, \pm 1,$$

in units of the ground-state hyperfine constant $g_0\mu_n H_{\text{eff}}$, where $\rho = g_1/g_0$ (for the case of $I_1 = I_0$, then $\rho = \mu_1/\mu_0$). Transforming to a normalized energy scale by

$$E_M'(m_1; m_0) = (E_{\text{max}} - E_{\text{min}})^{-1} \times [2E_M(m_1; m_0) - E_{\text{max}} - E_{\text{min}}],$$

one obtains relative-energy expressions from which a splitting diagram may be constructed. These equations, given in Ref. 2, for the 16 hyperfine lines between magnetic sublevels of states with $I_1 = I_0 = \frac{5}{2}$, are plotted in Fig. 6 as a function of ρ . This diagram holds for either sign of $g_0\mu_n H_{\text{eff}}$.

Comparison of the experimental velocity spectrum for NpAl_2 with the theoretical diagram for pure magnetic splitting shows that the sign of ρ is positive, because of the presence of the two weak outer lines. The symmetry of the diagram is such that the hyperfine pattern for any value of ρ is identical with that of its reciprocal; i.e., from line positions alone the magnetic-moment ratio can be determined, but it is impossible to determine which state has the larger moment. The values of ρ which best fit the NpAl_2 data are $+0.537$ and $+1.86$. For reasons to be discussed in the following section, it is possible to make an unambiguous choice

between these two values, to give

$$\rho = +0.537 \pm 0.005.$$

Using this value of ρ , and with $\kappa = 1$, the solid curve through the NpCl_4 data points in Fig. 5 was computed.

Nuclear Polarization Effect

Results of preliminary measurements are reported here on the observation of a nuclear polarization effect which permits selection of the correct value of ρ . At sufficiently low temperatures, when $g_0\mu_n H_{\text{eff}} \approx kT$, the populations of the different sublevels of the nuclear ground state, following the Boltzmann distribution, become unequal, giving nuclear polarization. This is manifested in the intensities of hyperfine lines in a Mössbauer spectrum. By observing the nuclear polarization effect in magnetically split Mössbauer spectra, the ambiguity in the magnetic-moment ratio between ρ and ρ^{-1} may be resolved, since there are significant qualitative differences in line intensities for the two cases. For NpAl_2 , the over-all hyperfine splitting is a sizable fraction of kT at 4.2°K ($5g_0\mu_n H_{\text{eff}} = 0.15 kT$). Therefore, an observable nuclear polarization effect is expected at the relatively high temperature of 4.2°K with NpAl_2 .

The behavior of the ground-state sublevel populations and the effect on Mössbauer line intensities at the extremes of high and low temperatures are illustrated

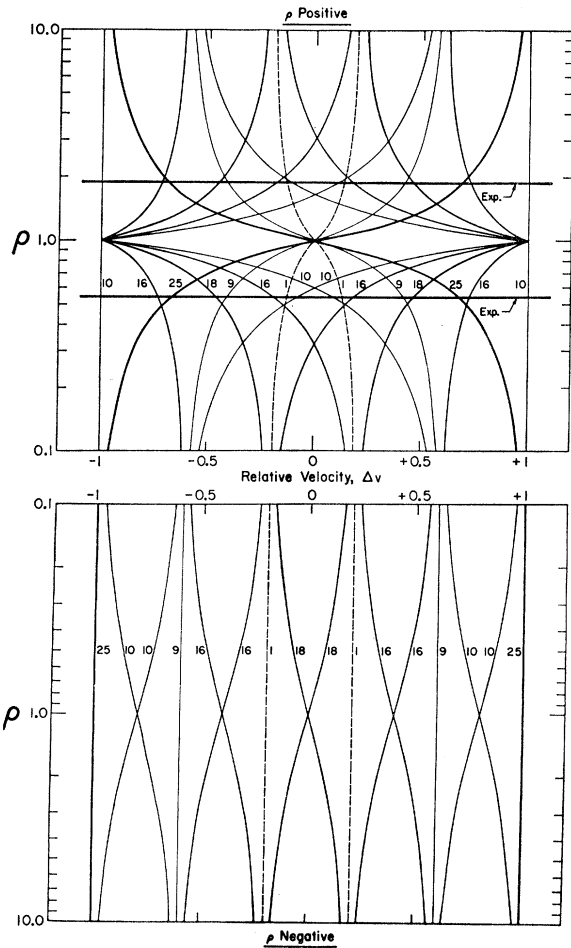


FIG. 6. Hyperfine line positions for $\frac{5}{2} \rightarrow \frac{5}{2}$ transitions with magnetic splitting, as a function of the magnetic-moment ratio ρ . Relative intensities are indicated for each line. Either horizontal line fits the experimental line positions for NpAl_2 at 4.2°K .

schematically in Fig. 7. For simplicity, only two transitions are shown, $-\frac{5}{2} \rightarrow -\frac{5}{2}$ and $+\frac{5}{2} \rightarrow +\frac{5}{2}$. At high temperatures ($g_0\mu_n H_{\text{eff}} \ll kT$), it is impossible to distinguish between the two cases ($\mu_0 > \mu_1$, or $\mu_0 < \mu_1$) because they give identical velocity spectra. However, at low temperatures ($g_0\mu_n H_{\text{eff}} \gg kT$), the behavior of the two cases is different. For $\mu_0 > \mu_1$, the more intense line is at the *higher* velocity, while for $\mu_0 < \mu_1$, it is at the *lower* velocity. When all 16 γ lines are considered, the effect of nuclear polarization is to weight the line intensities toward one side of the spectrum. The choice between the two cases is then reduced to the simple qualitative observation of whether the line intensities are weighted toward the higher or the lower velocities.

At 4.2°K , the magnetic splitting in NpAl_2 is expected to give 7–13% asymmetry in the intensities of the outermost lines. The velocity spectrum of NpAl_2 in Fig. 5 shows that the intensities are asymmetric and weighted toward the *higher* velocities. Thus, the choice of $\mu_0 > \mu_1$ is indicated for ^{237}Np . To confirm this choice,

TABLE II. Nuclear polarization effect in Mössbauer spectra of NpAl_2 .

Groups ^a	Intensity ratio at 4.2°K	Intensity ratio at 2.35°K	Experimental change	Calculated change
A/H	0.720 ± 0.015	0.628 ± 0.025	-0.092 ± 0.030	-0.094
B/G	0.834 ± 0.015	0.746 ± 0.025	-0.088 ± 0.030	-0.080
C/F	0.814 ± 0.015	0.774 ± 0.025	-0.040 ± 0.030	-0.039
D/E	1.019 ± 0.015	1.027 ± 0.025	$+0.008 \pm 0.030$	-0.018

^a Letters refer to groups of resonance lines labeled A through H in Fig. 5

the behavior of NpAl_2 was studied at 2.35°K ; at this lower temperature, the intensity asymmetry was expected to be even more pronounced toward the higher velocities. In Table II, the results of the experiments at 4.2 and 2.35°K are compared with calculated values. The lines in the NpAl_2 spectrum fall into eight groups, labeled A through H in Fig. 5; the area within each group, and thus the relative intensities, could be determined accurately by the least-squares fitting process. Intensity ratios between a group at low velocity and its counterpart group at high velocity are given in Table II; these are a measure of the asymmetry produced by nuclear polarization. Theoretical changes in asymmetry between 4.2 and 2.35°K were calculated from normalized intensities for each of the 16 γ lines, given for the i th γ line by

$$I_i = C_i \exp(-x) / \sum C_i \exp(-x),$$

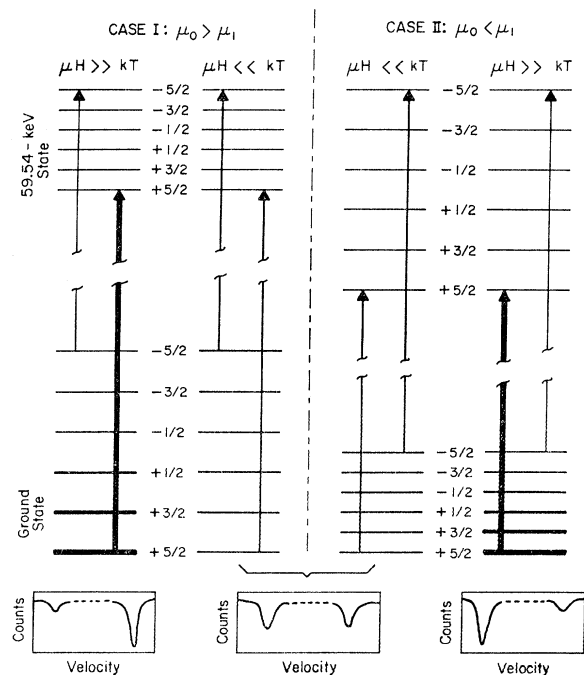


FIG. 7. Nuclear polarization effect on sublevel populations and absorption-line intensities. Relative populations are indicated by the thicknesses of the lines denoting the sublevels for high and low temperatures. The idealized Mössbauer spectra, shown as insets, illustrate the differences to be expected between Case I ($\mu_0 > \mu_1$) and Case II ($\mu_0 < \mu_1$).

where the C_i are proportional to the squares of Clebsch-Gordan coefficients, and $x = mg_0\mu_n H_{\text{eff}}/kT$; m is the magnetic quantum number of the sublevel from which the γ line arises. At 2.35°K the asymmetry increased toward the high velocities, with reasonably good agreement between the experimental and calculated values. The conclusion is that the magnetic moment of the ground state of ^{237}Np is larger than that of the 59.54-keV level, and that $\rho = 0.537$.

Nuclear polarization in a Mössbauer experiment was first demonstrated by Dash *et al.*,¹³ who used the large magnetic moment of ^{57}Co to produce polarization in the ^{57}Fe daughter. Large hyperfine splittings have been observed in Mössbauer experiments with other isotopes; for example, for ^{169}Tm metal at 5°K, Kalvius *et al.*¹⁴ observed the hyperfine splitting of the ground state to be about 2180 Mc. Their data exhibit the nuclear polarization effect in the enhanced intensities of γ lines arising from the lower ground-state sublevel. The unique application of nuclear polarization in the present work is the resolution of the ρ versus ρ^{-1} ambiguity at relatively high temperatures.

DISCUSSION

Comparison with Nuclear Theory

The measured values of κ and ρ may be compared with those predicted by the collective model of the nucleus,^{15,16} which is applicable to highly deformed nuclei such as ^{237}Np . Each intrinsic state is described by the quantum number K , the projection of the nuclear spin I on the nuclear symmetry axis, and by the set of asymptotic quantum numbers $[Nn_z\Lambda]$. (In the limit of large deformations, N is defined as the number of nodes in the nuclear wave function, n_z is the number of nodal planes perpendicular to the nuclear symmetry axis, and Λ is the projection of orbital angular momentum on this symmetry axis.) Thus, for ^{237}Np , the ground state is labeled $\frac{5}{2}[642]$, while the intrinsic state at 59.54 keV is $\frac{5}{2}[523]$. The magnetic moment of an intrinsic state is a property of the last unpaired nucleon in an odd- A nucleus, moving in a single-particle orbit described by $K[Nn_z\Lambda]$, and may be calculated from the appropriate wave function. The quadrupole moment, on the other hand, is a collective property of all the nucleons, directly related to the nuclear deformation parameter η . (The parameter η is defined by Nilsson¹⁵ to be positive for prolate deformations and negative for oblate deformations.) The equilibrium deformation, and thus the quadrupole moment, may be calculated by minimizing the sum of single-particle energies for all the nucleons;

¹³ J. G. Dash, R. D. Taylor, D. E. Nagle, P. P. Craig, and W. M. Visscher, *Phys. Rev.* **122**, 1116 (1961).

¹⁴ M. Kalvius, P. Kienle, H. Eicher, W. Wiedemann, and C. Schuler, *Z. Physik* **172**, 231 (1963).

¹⁵ S. G. Nilsson, *Kgl. Danske Videnskab. Selskab, Mat.-Fys. Medd.* **29**, No. 16 (1955).

¹⁶ B. R. Mottelson and S. G. Nilsson, *Kgl. Danske Videnskab. Selskab, Mat.-Fys. Skrifter* **1**, No. 8 (1959). See also K. Alder and R. M. Steffen, *Ann. Rev. Nucl. Sci.* **14**, 403 (1964).

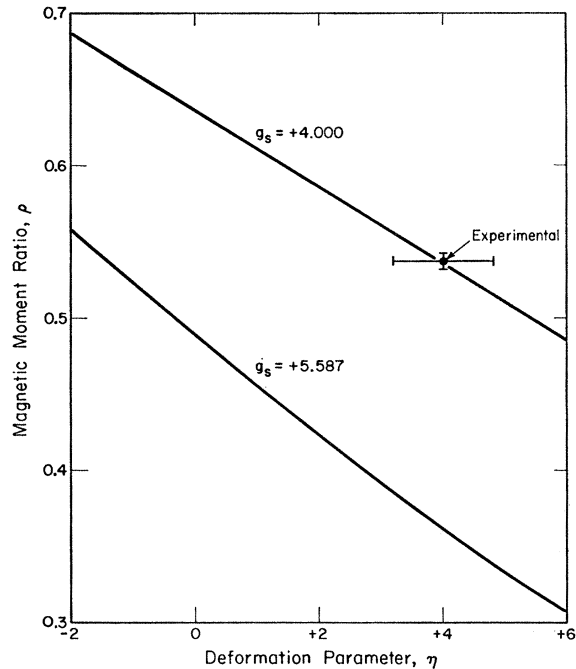


FIG. 8. Magnetic-moment ratio ρ as a function of nuclear deformation η , calculated from Nilsson wave functions for the $\frac{5}{2}[642]$ ground state and the $\frac{5}{2}[523]$ level at 59.54 keV in ^{237}Np . The lower curve gives the results of the calculation using the free-proton g factor ($g_s = +5.587$) for the odd nucleon; the upper curve is for a quenched nucleon g factor ($g_s = +4.000$). For the experimental point, the value of ρ is from the present work, while the experimental deformation is derived from Coulomb-excitation results.

it is not expected to be very sensitive to the state of the last unpaired nucleon. For ^{237}Np , this is borne out in the experimental value of κ , which shows that the quadrupole moments of the ground state and the 59.54-keV level are not very different. This gives experimental justification to the assumption, used in the magnetic-moment calculation that follows, that the two intrinsic states have the same deformation.

Collective-model magnetic moments have a contribution g_K associated with the intrinsic structure and another, g_R , associated with the collective rotation; the former depends upon the wave function of the last unpaired nucleon, while the latter does not. The magnetic moment,¹⁵ for $K \neq \frac{1}{2}$, is given by

$$\mu = (g_K - g_R)K^2(I+1)^{-1} + g_R I,$$

where

$$g_K = K^{-1}[(g_s - 1)(A^+ - \frac{1}{2}) + K]$$

for an odd-proton nucleus. Here A^+ is the probability, calculated from the nuclear wave function, that the spin of the odd proton is parallel to the nuclear symmetry axis. The parameter g_s is the g factor of the odd nucleon; as discussed below, it is generally somewhat less than the g factor of a free proton. For an intrinsic state with $I = K$,

$$\mu = (g_s - 1)(A^+ + G)I(I+1)^{-1},$$

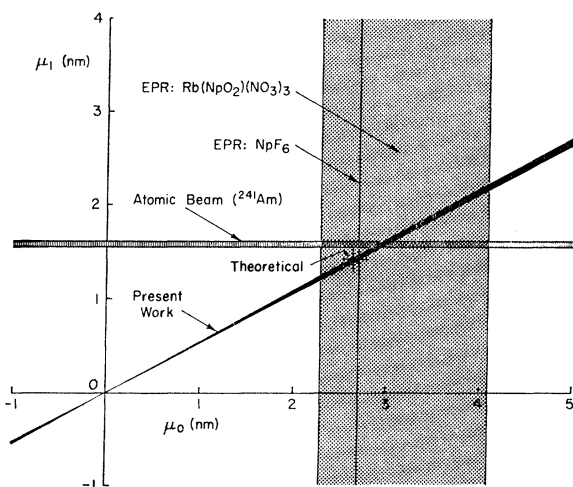


FIG. 9. Relationship of the magnetic-moment ratio determined in this work to other magnetic-moment measurements. Values for μ_0 and μ_1 predicted by the collective model (with quenched g_s) are also shown.

where

$$G = (g_R + I)(g_s - 1)^{-1} - \frac{1}{2}.$$

Then, the magnetic-moment ratio μ_1/μ_0 can be expressed as

$$\rho = (A_1^+ + G)(A_0^+ + G)^{-1}$$

when $K_1 = K_0$, as in the case of ^{237}Np .

Results of the calculation of A_1^+ , A_0^+ , and ρ as a function of deformation, using the tabulated wave functions of Nilsson,^{15,16} are given in Table III and Fig. 8 for different values of g_s . To a good approximation, g_R is given by Z/A or $93/237$; a recent atomic-beam measurement¹⁷ on ^{242}Am found $g_R \approx Z/A$, giving confidence in the use of this approximation in the heavy elements. The experimental deformation is taken from Coulomb-excitation work of Newton.¹⁸ Figure 8 shows that agreement with experiment is obtained when g_s is about 70% of the free-proton g factor. The concept of quenched nucleon magnetic moments in the collective model has successfully accounted for most of the magnetic moments that have been measured for deformed nuclei.^{19,20} In nearly all of these cases, quenched moments of 60–70% of the free-nucleon moment were required. Thus, the experimental value of ρ for ^{237}Np is consistent with the prediction of the collective model with a quenched proton magnetic moment.

¹⁷ L. Armstrong, Jr., and R. Marrus, *Phys. Rev.* **144**, 994 (1966).

¹⁸ J. O. Newton, *Nucl. Phys.* **5**, 218 (1958). A calculation of magnetic moments from Nilsson's wave functions for $\frac{5}{2}[642]$ and $\frac{5}{2}[523]$ states also appears in this paper. The principal difference in the present calculation is the use of revised wave functions from Ref. 16 for the $\frac{5}{2}[523]$ state.

¹⁹ J. O. Rasmussen and L. W. Chiao, in *Proceedings of the International Conference on Nuclear Structure, Kingston, Canada, 1960*, edited by D. A. Bromley and E. W. Vogt (The University of Toronto Press, Toronto, 1960), p. 646.

²⁰ J. De Boer and J. D. Rogers, *Phys. Letters* **3**, 304 (1963).

TABLE III. Values of A_1^+ and A_0^+ calculated from Nilsson wave functions.

	$\eta = -2$	$\eta = 0$	$\eta = +2$	$\eta = +4$	$\eta = +6$
A_1^+	0.316	0.272	0.236	0.197	0.160
A_0^+	0.669	0.690	0.728	0.771	0.814

Comparison with Other Data

The ground-state magnetic moment of ^{237}Np has been derived from paramagnetic-resonance data in two instances. A value for μ_0 of 3.2 ± 0.9 nm was calculated by Eisenstein and Pryce²¹ from the data of Bleaney *et al.*,²² on $\text{Rb}(\text{NpO}_2)(\text{NO}_3)_3$. From work on NpF_6 , Hutchinson and Weinstock²³ computed a value for μ_0 of 2.7 nm. The magnetic moment of the 59.54-keV level was measured by perturbed angular correlations to give μ_1 as $+2.0 \pm 0.5$ nm; however, known experimental difficulties make this value uncertain.²⁴ A better estimate of μ_1 can be obtained from the magnetic moment of ^{241}Am , whose ground state has the same $\frac{5}{2}[523]$ configuration; it has been measured directly in an atomic-beam experiment by Armstrong and Marrus¹⁷ as $+1.58 \pm 0.03$ nm.

This information is summarized in Fig. 9, where μ_0 is plotted against μ_1 , so that the true values of μ_0 and μ_1 will be represented by some single point on the graph. The results of the present work are given by a line with slope ρ . In addition to the measurements discussed above, which appear as vertical and horizontal bands, a point giving the result of the collective-model calculation (with quenched proton moment) is shown. In the absence of direct measurements of μ_0 and μ_1 , it is desirable to estimate them from the available evidence. From the converging information in Fig. 9, the following estimates appear to be reasonable:

$$\mu_1 \approx 1.5 \text{ nm},$$

$$\mu_0 \approx 2.8 \text{ nm}.$$

This estimate of μ_0 does not agree with the widely quoted value²² of 6.0 ± 2.5 nm. If μ_0 is 2.8 nm, the magnetic field at the nucleus is about 3×10^6 Oe in NpAl_2 and NpCl_4 .

ACKNOWLEDGMENTS

The authors wish to thank Dr. P. K. Smith for the preparation of NpAl_2 , Dr. D. G. Karraker for the preparation of NpCl_4 , and Mr. D. A. Brown for assistance in fabricating sources and absorbers.

²¹ J. C. Eisenstein and M. H. L. Pryce, *J. Res. Natl. Bur. Std.* **A69**, 217 (1965).

²² B. Bleaney, P. M. Llewellyn, M. H. L. Pryce, and G. R. Hall, *Phil. Mag.* **45**, 992 (1954).

²³ C. A. Hutchinson, Jr., and B. Weinstock, *J. Chem. Phys.* **32**, 56 (1960).

²⁴ V. E. Krohn, T. B. Novey, and S. Raboy, *Phys. Rev.* **98**, 1187 (1955); **105**, 234 (1956).